Scientific Report

SOURCE DATA | TRANSPARENT PROCESS | OPEN ACCESS

EMBO reports

Cabut/dTIEG associates with the transcription factor Yorkie for growth control

Marina Ruiz-Romero[1], Enrique Blanco[1,2], Nuria Paricio[3], Florenci Serras[1] & Montserrat Corominas[1,*]

Abstract

The *Drosophila* transcription factor Cabut/dTIEG (Cbt) is a growth regulator, whose expression is modulated by different stimuli. Here, we determine Cbt association with chromatin and identify Yorkie (Yki), the transcriptional co-activator of the Hippo (Hpo) pathway as its partner. Cbt and Yki co-localize on common gene promoters, and the expression of target genes varies according to changes in Cbt levels. Down-regulation of Cbt suppresses the overgrowth phenotypes caused by mutations in *expanded* (*ex*) and *yki* overexpression, whereas its up-regulation promotes cell proliferation. Our results imply that Cbt is a novel partner of Yki that is required as a transcriptional co-activator in growth control.

Keywords Cabut; dTIEG; GAF; growth; Yorkie
Subject Categories Development & Differentiation; Transcription
DOI 10.15252/embr.201439193 | Received 20 June 2014 | Revised 24 November 2014 | Accepted 8 December 2014 | Published online 8 January 2015
EMBO Reports (2014) 16: 362–369

Introduction

Gene expression is regulated through the integrated action of, among others, many cis-regulatory elements, including core promoters and enhancers located at greater distances from transcription start sites (TSS) (reviewed in [1]). The combinatorial binding of transcription factors (TF) to these elements can lead to diverse types of transcriptional output, and an understanding of this mechanism is crucial, for example, in the context of development. In fact, the final size and shape of an organism require a complex genetic network of signaling molecules, the final outcome of which must be finely regulated in space and time to ensure a proper response.

The transcription factor Cabut/dTIEG (Cbt) is the fly ortholog of TGF-β-inducible early genes 1 and 2 (TIEG1 and TIEG2) in mammals, which belong to the evolutionary conserved TIEG family [2]. TIEGs are zinc finger proteins of the Krüppel-like factor (KLF) family that can function as either activators or repressors depending on the cellular context, the promoter to which they bind or the interacting partners [3]. TIEG proteins participate in a wide variety of cellular processes, from development to cancer, and regulate genes that control proliferation, apoptosis, regeneration or differentiation [4,5].

Drosophila cbt was identified and characterized from an overexpression screen of EP lines conducted to determine genes involved in establishing epithelial planar cell polarity [6,7]. This TF is ubiquitously expressed in the wing disk, and its expression increases in response to metabolic, hormonal and stress signals. *Cbt* levels rise upon inhibition of TOR signaling [8,9], and it is among the most highly Mlx-regulated genes [10]. Among its functions, it is known that Cbt is required during dorsal closure downstream of JNK signaling [7], that it is a modulator of different signaling pathways involved in wing patterning and proliferation [11] and that it promotes ectopic cell cycling when overexpressed [12]. Moreover, Cbt is a crucial downstream mediator gene of the JNK signaling required during wing disk regeneration [5]. In spite of this, little is known about its downstream target genes or its precise mechanism of action. Here, we report a novel function for Cbt as a partner of Yki (Yorkie). Yki is the key effector of growth control and the downstream element of the highly conserved Hpo (Hippo) signaling pathway. The Hpo pathway limits organ size by phosphorylating and inhibiting Yki, a key regulator of proliferation and apoptosis. Yki can also act as an oncogene, since it has potent growth-promoting activity (reviewed in [13]). Our results show a role for Cbt as a transcriptional activator with the capacity to modulate Yki growth response.

Results and Discussion

Widespread occupancy of Cbt on chromatin

To characterize Cbt target genes, we performed chromatin immunoprecipitation and high-throughput sequencing (ChIP-Seq) from third instar larval wing imaginal disks [14,15]. Analysis of Cbt-bound regions (Supplementary Table S1) in the entire genome revealed that approximately 70% of its peaks were located in proximal promoters or introns (Fig 1A and B and Supplementary Fig S1A), consistent with its role as a transcriptional regulator. Thus, we identified 2,060 putative target genes in the wing disk (Supplementary Table S2). Gene Ontology (GO) [16] analysis indicated that this

1 Departament de Genètica, Facultat de Biologia and Institut de Biomedicina (IBUB) de la Universitat de Barcelona, Barcelona, Spain
2 Centre for Genomic Regulation (CRG), Barcelona, Spain
3 Departamento de Genética, Facultad de Ciencias Biológicas, Universidad de Valencia, Valencia, Spain
*Corresponding author. Tel: +34 93 4037003; E-mail: mcorominas@ub.edu

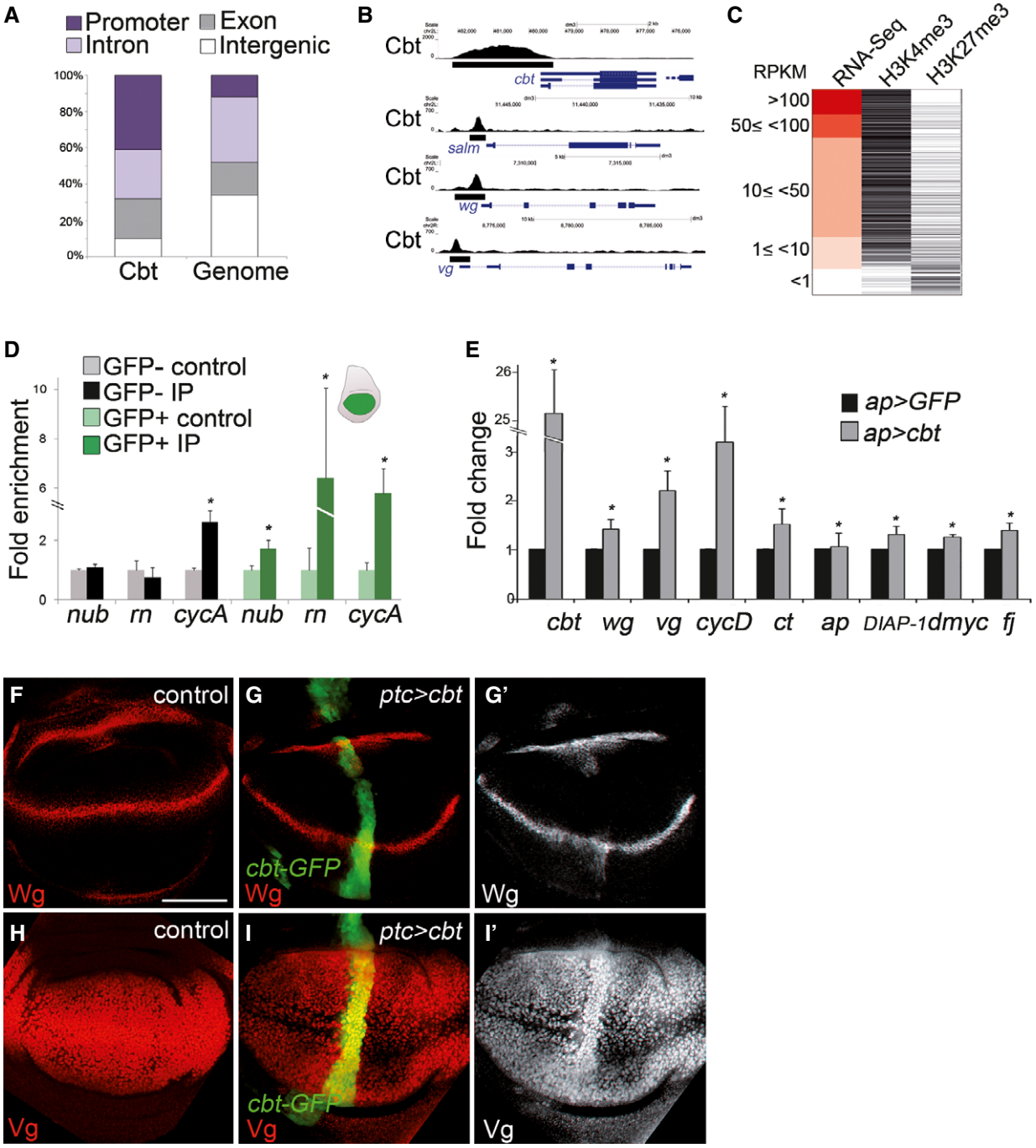

Figure 1. Cbt occupancy correlates with actively transcribed genes.

A Genome distribution of Cbt peaks (left). Coverage of each class of gene region in the entire genome (right). Cbt peaks are preferentially located in promoter regions (from −1,000 to 100 bp from the TSS).

B UCSC genome browser screenshot of the Cbt ChIP-Seq profile across regions of known (*cbt* and *salm*) and unknown targets (*wg* and *vg*). The height of the profile represents the number of reads, and peaks are depicted as black boxes.

C Ranking of Cbt target genes according to their expression from RNA-Seq in wing imaginal disk (left). Heatmap (right) showing the presence (black) and absence (white) of H3K4me3 and H3K27me3 histone modifications on these genes (data from[15]).

D Cbt ChIP analysis of GFP-negative cells (GFP^-, black) and GFP-positive cells (GFP^+, green) from sorted *nub-Gal4; UAS-GFP* wing disks. Control samples (mock) of GFP^- (gray) and GFP^+ (light green). Real-time PCR results were normalized against the mock sample (negative) and are depicted as fold enrichment. Error bars represent the SEM. *T*-test (*)$P \leq 0.05$, $n = 3$.

E Comparison of mRNA expression levels of identified Cbt target genes quantified by real-time PCR in wt (wild-type) (black) and *ap > cbt* (gray) wing disks. Error bars represent SEM. *T*-test (*)$P \leq 0.05$, $n = 4$.

F–I (F and H) Wg and Vg (red) staining in wt disks (control). (G and I) Ectopic *cbt* expression in the medial region of the wing disk using *ptc-GAL4* (green) induces up-regulation of Wg (G-G', red) and Vg (I-I', red) in the wing pouch. Scale bar = 50 μm.

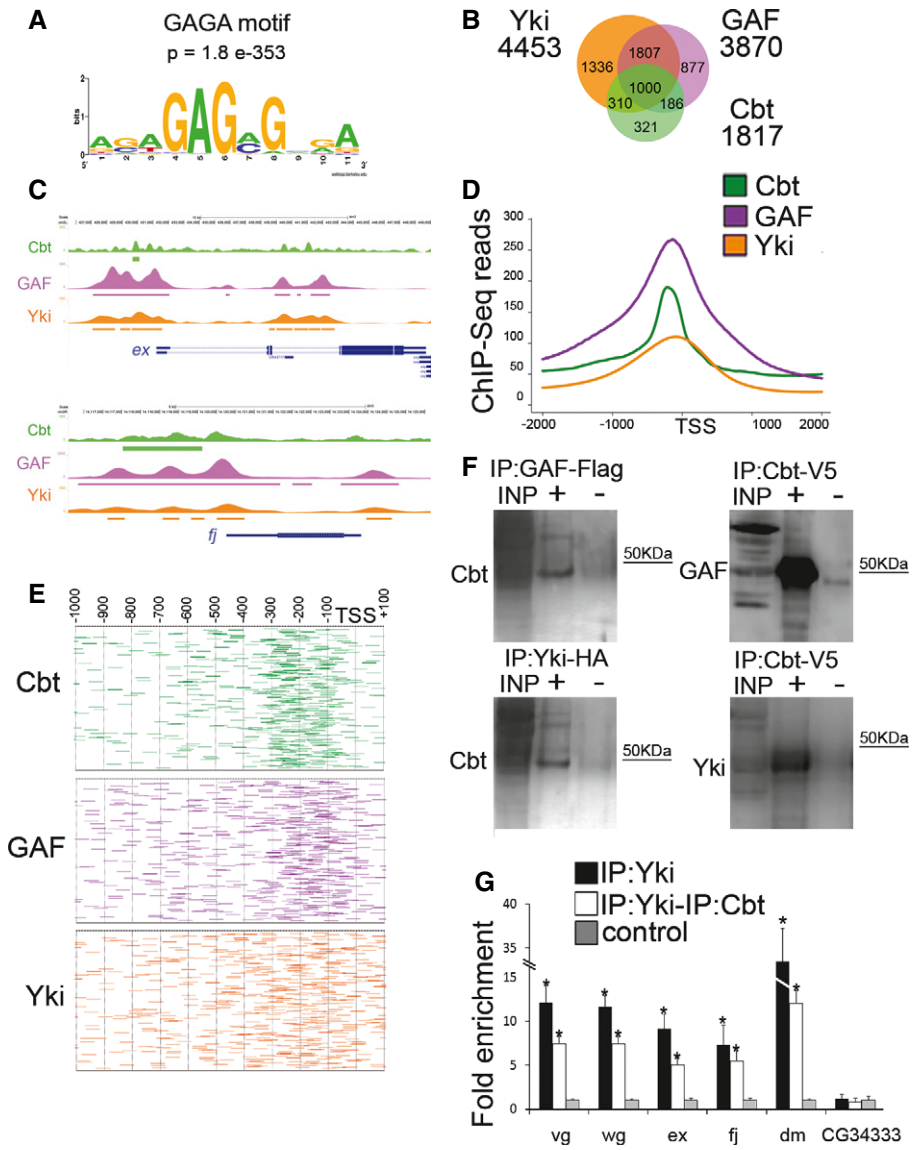

Figure 2. Cbt occupancy overlaps with GAF and Yki binding in the genome.

A Motif and significance score for GAF DNA-binding protein at Cbt-bound targets. *De novo* analysis with MEME-ChIP identified GAF motif (GAGA) as one of the most representative motifs enriched within Cbt binding regions.

B Venn diagram showing the overlap between Cbt (green), GAF (purple) and Yki (orange) in the promoters of their target genes.

C UCSC Genome Browser overview of Cbt (green), GAF (purple) and Yki (orange) ChIP-Seqs in *ex* and *fj* regions. Peaks are represented as boxes in different colors: Cbt (green), GAF (purple) and Yki (orange).

D Distribution of Cbt (green), GAF (purple) and Yki (orange) ChIP-Seq reads over the TSS of common target genes.

E Distribution of Cbt (green), GAF (purple) and Yki (orange) location in the promoters of their target genes.

F Western blots showing proteins immunoprecipitated from S2 cells transfected with Yki-HA, GAF-Flag or Cbt-V5 cells and detected by anti-Cbt, anti-GAF and anti-Yki antibodies. Input (INP), immunoprecipitated samples (+) and negative control (−).

G ChIP-reChIP of Yki-HA and Cbt from S2 cells tested by real-time PCR. The order of antibodies is Yki-HA ChIP and Cbt. Yki-HA ChIP (black), ChIP-reChIP (white). CG34333 promoter region was used as a negative bound region, and results were normalized against input and the mock sample (negative control, gray) and are depicted as fold enrichment. Error bars represent fold enrichment error. *T*-test (*)$P \leq 0.05$, $n = 3$.

Source data are available online for this figure.

subset of genes was enriched in transcriptional activity, cell migration, mitotic cell cycle and signaling pathways known to play a role in imaginal disk development (Supplementary Fig S1B). As expected, among Cbt targets we found previously described genes such as *salm* (*spalt major*) or *cbt* itself [11,17], but also several unidentified target genes such as *wg* (*wingless*) or *vg* (*vestigial*) (Fig 1B).

Cbt association around the TSS may be an indication of its function as a primary regulatory element, but does not provide any information about its role as an activator or a repressor. To

elucidate this question, we examined published data on chromatin modifications [15] as well as recently obtained RNA-Seq data from the wing disk (Pérez-Lluch, in preparation) and ranked Cbt targets according to their expression level (Fig 1C). Although at different levels, target genes are mostly expressed in the wing disk. This positive correlation with gene expression was also detected in the extensive overlap between Cbt occupancy and trimethylated histone 3 lysine 4 (H3K4me3). In contrast, only 13% of Cbt target genes correlated with the repressive chromatin mark H3K27me3 (Supplementary Fig S1C–G). Although 200 Cbt targets seemed to present both modifications, these may be coupled to the differential expression pattern of several genes in the wing disk. To clarify whether Cbt binds to active or inactive genes, we next examined Cbt occupancy of genes known to be differentially expressed in a subpopulation of cells within the wing disk tissue. The gene *nub* (*nubbin*) is expressed in the wing primordium [18]. We induced GFP expression in the wing pouch using a *nub-GAL4* driver and performed ChIP assays followed by quantitative PCR (qPCR) in sorted cells (Fig 1D and Supplementary Fig S1E). In the vicinity of the TSS of genes expressed in the wing pouch, such as *rn* (*rotund*) and *nub*, we only found Cbt in GFP-positive cells. Cbt was also present in the promoter of *cycA* (*cyclin A*), both in GFP-positive and GFP-negative cells, in accordance with its expression throughout the entire wing disk (wing pouch and notum). These observations indicate that Cbt might act as a positive activator of transcription in this tissue. To further confirm this, we examined the expression of selected targets after *cbt* overexpression. Induction of *cbt* in the dorsal domain of the wing using an *ap-GAL4 (apterous)* driver led to a clear increase in the expression levels of target genes, as detected by qPCR (Fig 1E). We also ectopically expressed *cbt* in the *ptc* (*patched)* domain of the wing disk using the *ptc-GAL4* driver and examined the pattern of Wg (normally restricted to cells adjacent to the D/V boundary in the wing blade and to two rings in the hinge region) and Vg (expressed throughout the wing blade) by immunostaining. After *cbt* induction, we observed spread staining of Wg in the boundary and ring regions (Fig 1F–G'). Likewise, analysis of Vg revealed increased protein levels in the region where *cbt* was upregulated (1H–I'). No ectopic expression of Wg or Vg was detected in regions far from where they are normally expressed, suggesting that *cbt* alone is not sufficient to ectopically activate transcription of these genes but can modulate or cooperate with factors that promote their basal expression. Taken together, our results suggest that Cbt functions as a transcriptional activator in the wing disk. Nevertheless, we cannot discard its contribution to repression in some contexts or through binding to different partners, as previous experiments have demonstrated the relevance of the Sin3A interaction domain for Cbt's repressive role [17].

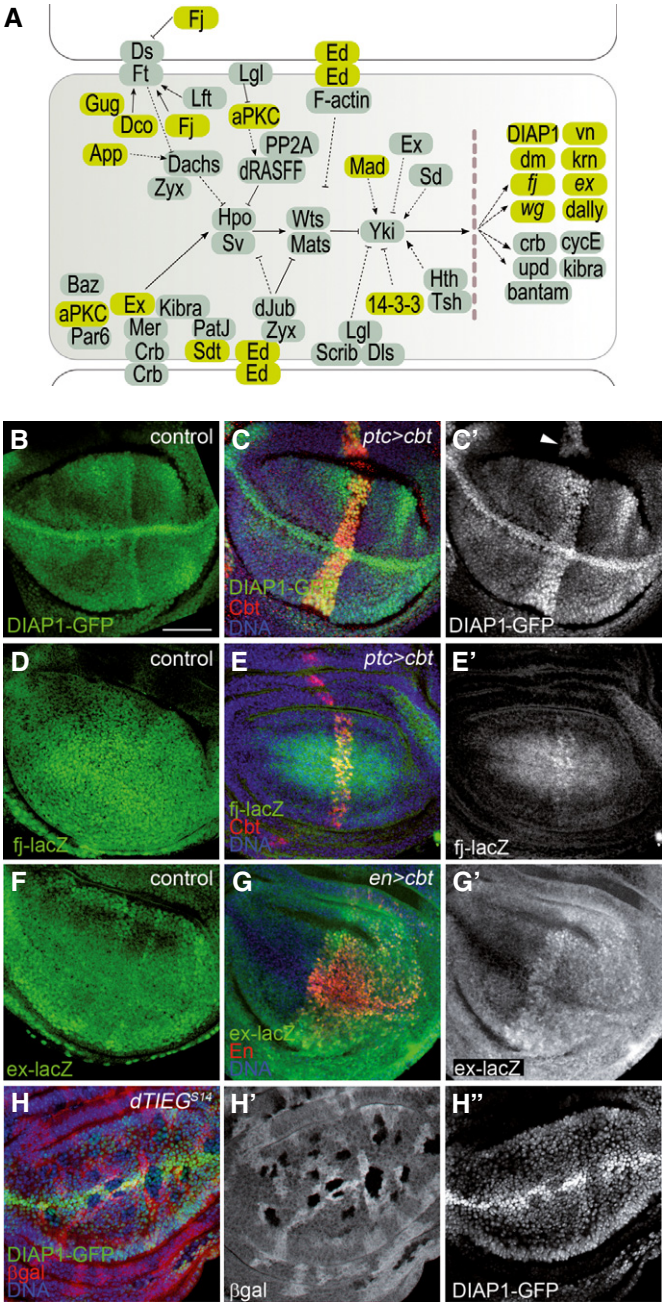

Figure 3. Influence of Cbt on the expression of Yki target genes.

A Representation of the Hpo pathway and Yki target genes (according to the Kegg pathway [36]). Genes identified as Cbt targets that belong to the pathway are highlighted in green.

B–G Expression pattern of *DIAP1*, *fj* and *ex* reporters after overexpressing *cbt* (red) in wing disks. Scale bar = 50 μm. (B–C') *DIAP1-GFP* expression in *wt* (control, B) and *ptc>cbt disks* (C–C'). (D–E') *fj-lacZ* expression (green) in *wt* (control, D) and *ptc > cbt disks* (E–E'). (F–G') *ex-lacZ* expression in *wt* (control, F) and *en > cbt disks* (G–G').

H Analysis of *DIAP1-GFP* (green) in *cbt* mutant clones (*dTIEG^{S14}*, *black*).

Cbt associates with GAF and Yki proteins

TIEG factors contain three conserved C-terminal zinc finger motifs that seem to bind to GC-rich sequences in vertebrates [19–22]. To characterize the set of motifs enriched within Cbt binding sites, we used different pattern discovery methods (see Materials and Methods, Supplementary Fig S2 and Supplementary Table S3). Among others, we detected GC sequences and the Sp1 motif, as expected for a TIEG family member, but in addition, one of the most enriched motifs comprised GAGA-binding sequences (Fig 2A). We did not find enrichment of the proposed consensus TIEG motif

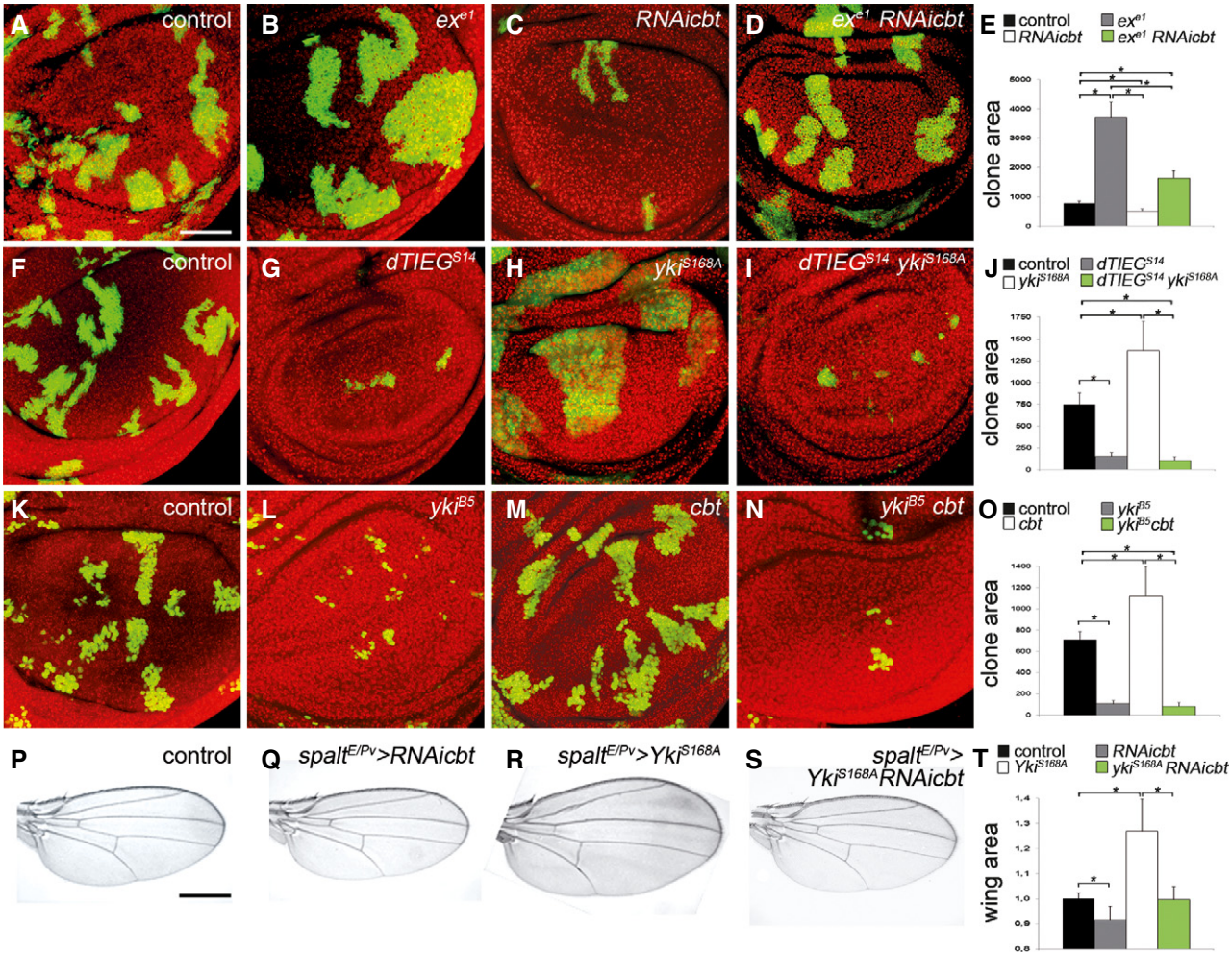

Figure 4. Cbt is required for Yki activity in wing development.

A–E Wing disks containing GFP-marked MARCM clones of the ex^{e1} mutant allele (B), *cbt* RNAi (C) and ex^{e1} mutant clones with *cbt* RNAi (D). Scale bar = 50 μm. (E) Quantification of clone area of control (black), *ex* mutant (gray), *cbt* RNAi (white) and ex^{e1} clones with *cbt* RNAi (green). Error bars represent SEM. *T*-test (*)$P \leq 0.003$, $n = 10$.

F–J Wing disks containing GFP-marked MARCM clones of the $dTIEG^{S14}$ mutant allele (G), Yki^{S168A} overexpression (H) and $dTIEG^{S14}$ mutant clones with yki^{S168A} overexpression (I). (J) Quantification of clone area of control (black), *cbt* mutant (gray), *yki* overexpression (white) and *cbt* mutant with *yki* overexpression (green). Error bars represent SEM. *T*-test (*)$P \leq 0.0003$, $n = 10$.

K–O Wing disks containing GFP-marked MARCM clones of the yki^{B5} mutant allele (L), *cbt* overexpression (M) and yki^{B5} mutant clones with *cbt/dTIEG* overexpression (N). (L) Quantification of clone area of control (black), *yki* mutant (gray), *cbt* overexpression (white) and *yki* mutant with *cbt* overexpression (green). Error bars represent SEM. *T*-test (*)$P \leq 0.004$, $n = 10$.

P–T Wings expressing *cbt* RNAi (R), yki^{S168A} (Q) and yki^{S168A} with *cbt* RNAi (S) under $spalt^{E/Pv}$ promoter for 24 h. Scale bar = 0.5 mm. (T) Quantification of wing area of control (black) *cbt* RNAi (gray), yki^{S168A} (white) and *cbt* RNAi with yki (green). Error bars represent SD. *T*-test (*)$P \leq 0.00001$, $n = 50$.

5′GGTGTG3′ [23], which suggests that Cbt binds to degenerated or alternative motifs or may function through its interaction with other TFs. A recent study identified a novel Mad-like motif in promoters of Cbt-regulated genes [12]. However, this new motif does not coincide with previously reported Cbt binding data [17,24].

Association of Cbt genome occupancy with regions bound by other TFs expressed in wing disk using reported data [25] showed strong correlations between Cbt, Yki and the general factor GAF (GAGA factor) (Fig 2B). More than 70% of Cbt targets were also Yki targets, and of these, around 76% were occupied by the three of them (Fig 2B). Fig 2C shows the profiles of these factors in known Yki targets such as *ex* (*expanded*) and *fj* (*four-jointed*). Mapping the targets on common gene promoters revealed that most of Cbt and GAF were located mainly at the promoter region close to the TSS (Fig 2E). Although this distribution was more scattered in the case of Yki, the majority of targets were observed in the same region. Projection of the mean reads over the TSS of the full set of genes confirmed this observation (Fig 2D). Analysis of Cbt and GAF in polytene chromosomes confirmed their co-localization in particular bands (Supplementary Fig S3A and B). The interaction of Cbt with Yki and GAF proteins was confirmed by co-immunoprecipitation in S2 cells. Western blotting revealed that Cbt specifically co-precipitate with Yki and GAF (Fig 2F and

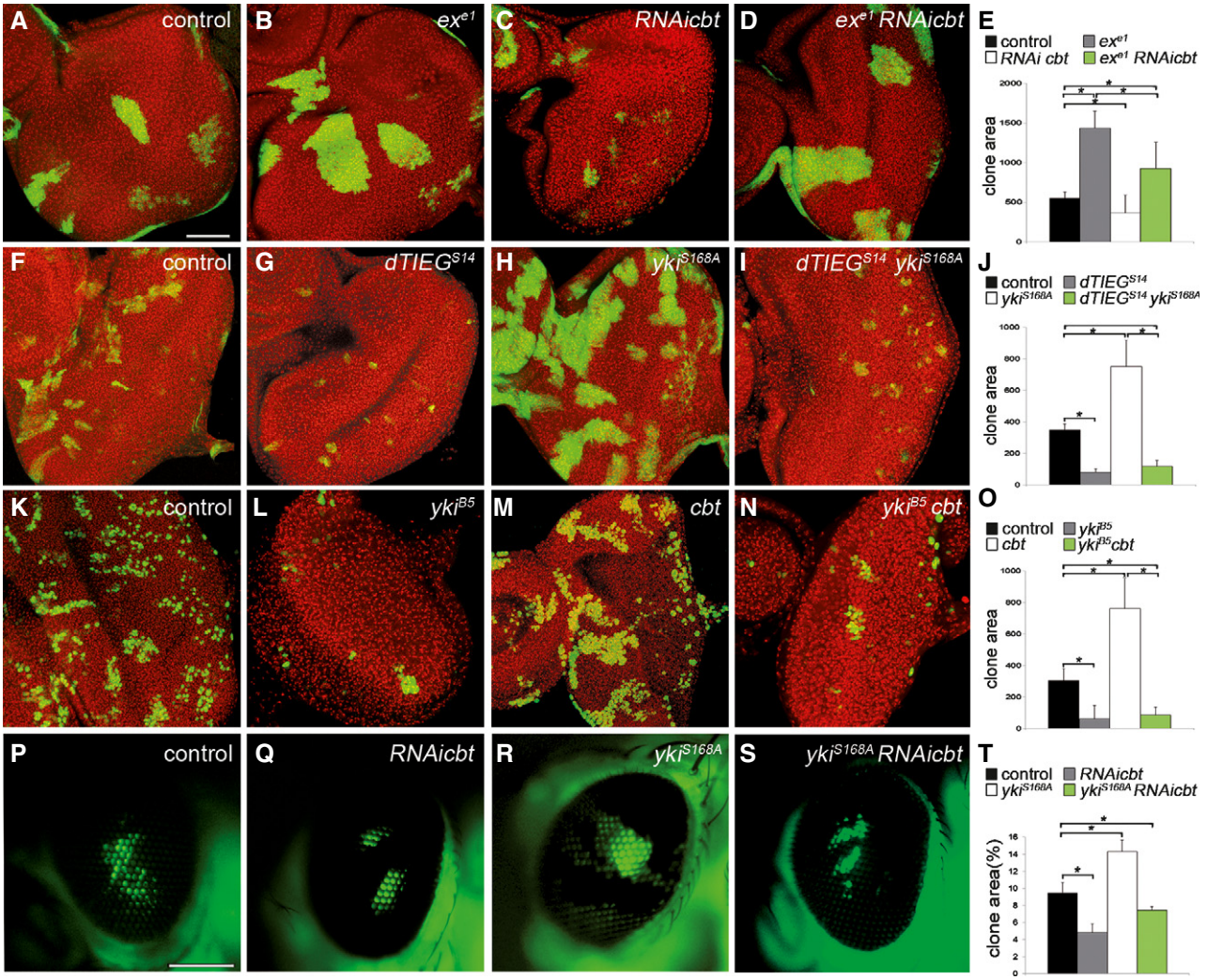

Figure 5. Cbt is required for Yki activity in eye development.

A–E Eye disks containing GFP-marked MARCM clones of the ex^{e1} mutant allele (B), *cbt* RNAi (C) and ex^{e1} mutant clones with *cbt* RNAi (D). Scale bar = 50 μm. (E) Quantification of clone area of control (black), *ex* mutant (gray), *cbt* RNAi (white) and *ex* mutant with *cbt* RNAi (green). Error bars represent SEM. *T*-test (*) $P \leq 0.05$, $n = 10$.

F–J Eye disks containing GFP-marked MARCM clones of the $dTIEG^{S14}$ mutant allele (G), Yki^{S168A} overexpression (H) and $dTIEG^{S14}$ mutant clones with yki^{S168A} overexpression (I). (J) Quantification of clone area of control (black), *cbt* mutant (gray), *yki* overexpression (white) and *cbt* mutant with *yki* overexpression (green). Error bars represent SEM. *T*-test (*) $P \leq 0.03$, $n = 10$.

K–O Eye disks containing GFP-marked MARCM clones of the yki^{B5} mutant allele (L), *cbt* overexpression (M) and yki^{B5} mutant clones with *cbt* overexpression (N). (L) Quantification of clone area of control (black), *yki* mutant (gray), cbt overexpression (white) and *yki* mutant with *cbt* overexpression (green). Error bars represent SEM. *T*-test (*) $P \leq 0.0001$, $n = 10$

P–T Eyes containing clones expressing *cbt* RNAi (R), yki^{S168A} (Q) and yki^{S168A} with *cbt* RNAi (S). Scale bar = 400 μm. (T) Quantification of the percentage occupied for eye clone area from the whole eye, of control (black) *cbt* RNAi (gray), yki^{S168A} (white) and *cbt* RNAi with yki (green). Error bars represent SEM. *T*-test (*) $P \leq 0.02$, $n = 10$.

Supplementary Fig S3C). To finally verify co-binding of Cbt and Yki in specific targets, we used the ChIP-reChIP technique and found that both factors bind in close vicinity on the same regions (Fig 2G), which confirms they physically interact. Altogether, our data suggest that Cbt, GAF and Yki act together to regulate gene transcription. Whether this interaction is direct or mediated by other proteins remains to be elucidated.

Close inspection of members of the Hpo pathway showed that several upstream and downstream components were Cbt targets (Fig 3A). To further investigate the requirement of Cbt in controlling Yki target genes expression, we examined the levels of *fj*, *DIAP1* (*Drosophila inhibitor of apoptosis*) and *ex* under conditions of elevated or reduced expression of *cbt*. *fj*, *DIAP1* and *ex* reporters exhibited higher levels in the *cbt* overexpression domains (Fig 3B–G'), whereas loss-of-function clones showed reduced *DIAP1* expression (Fig 3H) and *fj* levels decreased in the presence of *cbt* RNAi (Supplementary Fig S3E). As expected, and consistent with the occupancy profile, no changes were observed in the expression of *bantam*, a component of the Yki pathway not bound by Cbt (Supplementary Fig S3G).

Many studies have emphasized the complexity of Yki and its mammalian homologs YAP and TAZ regulation, including multiple combinations with associate proteins in distinct target genes (reviewed in [13]). Besides DNA-binding partners such Sd (Scalloped) and Hth (Homothorax) in *Drosophila* [26,27], Yki can cooperate with other factors directly on target promoters, such as the cell cycle-related gene dE2F1 [28]. Remarkably, a recent report shows that Cbt and dE2F1 regulate an overlapping set of cell cycle genes [12]. In the Dpp pathway, Mad (Mothers against decapentaplegic) and Yki interact to form a transcription complex to activate their common targets [29]. This association is conserved through evolution, as YAP and TAZ interact with Smad proteins to potentiate transcriptional activity [30]. Recent studies have also identified Mask (Multiple ankyrin repeats single KH domain) as a novel cofactor for Yki/YAP, required to induce target gene expression [31,32]. Our results highlight the role of Cbt as a new Yki partner involved in the activation of some Yki target gene expression. This function of Cbt may occur in part through association with GAF as well as chromatin remodeler complexes [25].

Cbt modulates Yki activity

Since overexpression of *cbt* results in an increase in proliferation as well as wing size [11] (Supplementary Fig S4), we hypothesized that Cbt's role in size control could be mediated through its association with Yki. To address this question, we depleted *cbt* levels and analyzed the effect on the growth of *ex* mutant clones and in clones overexpressing *yki* in wing and eye-antenna imaginal disks. The Yki target gene *ex* acts as an upstream positive modulator of the Hpo pathway, and in accordance with its role as a tumor suppressor, its loss-of-function mutation results in large clones (Figs 4B and 5B) [33]. Expression of *cbt* RNAi in this mutant background caused a clear reduction in the clone size (Figs 4D, 5D and Supplementary Fig S5). In the same direction, the overgrowth known to occur by overexpression of a *yki*-activated form (Figs 4H and 5H) [34] is prevented in a mutant *cbt* background (Figs 4I and 5I) as well as expressing *cbt* RNAi (Fig 4S and Supplementary Fig S5). Moreover, impaired growth caused by *yki* depletion could not be rescued increasing *cbt* levels (Figs 4K–O and 5K–O) and overexpression of *yki* and *cbt* triggered massive growth in imaginal tissues (Supplementary Fig S5). Finally, depletion of *cbt* in adult organs (wings and eyes) also reduced Yki-mediated overgrowth (Figs 4P–T and 5P–T), indicating a general function for Cbt in the regulation of Hippo pathway-mediated tissue growth.

In addition to its role during development, it has been shown that Cbt expression is highly regulated by stress and metabolic conditions [9,10]. Cbt has also been identified as a JNK-inducible gene during dorsal closure [7], and we have shown that JNK and tissue damage trigger *cbt* transient overexpression to promote wing disk regeneration, indicating that its levels must be finely controlled during regenerative growth [5]. Moreover, *cbt* heterozygous mutant disks fail to proliferate and do not regenerate [5], and it is known that during regeneration, the JNK pathway triggers Yki translocation to the nucleus to promote the proliferative response [35]. Altogether, our data support a model for Cbt acting as a modulator of Yki activity in the transcriptional regulatory mechanisms that control tissue growth.

Materials and Methods

ChIP-Seq

Cbt ChIP-Seq from wing imaginal disks was performed using a specific antibody against Cbt [14]. One thousand four-hundred disks from *Canton S* third instar larva were pooled and used as a source of chromatin as described [15]. IP buffer and 2 μl of Cbt/dTIEG antibody were used for immunoprecipitation. Immunoprecipitated and input samples were processed and sequenced following Solexa/Illumina protocols at the Ultrasequencing Unit of the CRG (Barcelona, Spain). 8 ng of each sample was used, and fragments between 300 and 350 bp were size-selected before sequencing. ChIP-Seq profiles and target regions were deposited in NCBI GEO under the accession number GSE40958.

Cell sorting and real-time PCR

Five hundred dissected disks were dissociated after incubation in trypsin solution for 1 h. Cells were collected in Schneider medium with DAPI and sorted by a cytometer. Recovered cells were then processed for chromatin immunoprecipitation as previously described [15]. IP buffer and 2 μl of Cbt antibody were used. Real-time PCRs were normalized against the mock (negative) sample and depicted as fold enrichment.

Supplementary information for this article is available online: http://embor.embopress.org

Acknowledgements
We thank N. Tapon for stocks, plasmids and insightful suggestions, J. Bernués for plasmids and GAF antibody, KD. Irvine for Yki antibody, S. Pérez-Lluch for ChIP-Seq and cell sorting support and M. Milán and I. Rodríguez for stocks. We also thank the Confocal Unit of the CCiTUB (Universitat de Barcelona) and M. Bosch for help with image analysis. M.R.R. was supported by a FPI fellowship, and this project was funded by Grants BFU2009-09781, CSD2007-00008 and BFU2012-36888, Ministerio de Economía y Competitividad, Spain.

Author contributions
MR-R, FS and MC designed the project and analyzed results; MR-R performed the experiments; EB performed computational analysis; NP provided materials, reagents and insightful discussions; and MR-R and MC wrote the manuscript.

Conflict of interest
The authors declare that they have no conflict of interest.

References

1. Lenhard B, Sandelin A, Carninci P (2012) Metazoan promoters: emerging characteristics and insights into transcriptional regulation. *Nat Rev Genet* 13: 233 – 245
2. Munoz-Descalzo S, Belacortu Y, Paricio N (2007) Identification and analysis of cabut orthologs in invertebrates and vertebrates. *Dev Genes Evol* 217: 289 – 298
3. Kim J, Shin S, Subramaniam M, Bruinsma E, Kim TD, Hawse JR, Spelsberg TC, Janknecht R (2010) Histone demethylase JARID1B/KDM5B is a corepressor of TIEG1/KLF10. *Biochem Biophys Res Commun* 401: 412 – 416

4. Subramaniam M, Hawse JR, Johnsen SA, Spelsberg TC (2007) Role of TIEG1 in biological processes and disease states. *J Cell Biochem* 102: 539 – 548
5. Blanco E, Ruiz-Romero M, Beltran S, Bosch M, Punset A, Serras F, Corominas M (2010) Gene expression following induction of regeneration in Drosophila wing imaginal discs. Expression profile of regenerating wing discs. *BMC Dev Biol* 10: 94
6. Rorth P, Szabo K, Bailey A, Laverty T, Rehm J, Rubin GM, Weigmann K, Milan M, Benes V, Ansorge W *et al* (1998) Systematic gain-of-function genetics in Drosophila. *Development* 125: 1049 – 1057
7. Munoz-Descalzo S, Terol J, Paricio N (2005) Cabut, a C2H2 zinc finger transcription factor, is required during Drosophila dorsal closure downstream of JNK signaling. *Dev Biol* 287: 168 – 179
8. Guertin DA, Guntur KV, Bell GW, Thoreen CC, Sabatini DM (2006) Functional genomics identifies TOR-regulated genes that control growth and division. *Curr Biol* 16: 958 – 970
9. Bulow MH, Aebersold R, Pankratz MJ, Junger MA (2010) The Drosophila FoxA ortholog Fork head regulates growth and gene expression downstream of Target of rapamycin. *PLoS ONE* 5: e15171
10. Havula E, Teesalu M, Hyötyläinen T, Seppälä H, Hasygar K, Auvinen P, Orešič M, Sandmann T, Hietakangas V (2013) Mondo/ChREBP-Mlx-regulated transcriptional network is essential for dietary sugar tolerance in Drosophila. *PLoS Genet* 9: e1003438
11. Rodriguez I (2011) Drosophila TIEG is a modulator of different signalling pathways involved in wing patterning and cell proliferation. *PLoS ONE* 6: e18418
12. Song M, Zhang Y, Katzaroff AJ, Edgar BA, Buttitta L (2014) Hunting complex differential gene interaction patterns across molecular contexts. *Nucleic Acids Res* 42: e57
13. Oh H, Irvine KD (2010) Yorkie: the final destination of Hippo signaling. *Trends Cell Biol* 20: 410 – 417
14. Belacortu Y, Weiss R, Kadener S, Paricio N (2011) Expression of Drosophila Cabut during early embryogenesis, dorsal closure and nervous system development. *Gene Expr Patterns* 11: 190 – 201
15. Perez-Lluch S, Blanco E, Carbonell A, Raha D, Snyder M, Serras F, Corominas M (2011) Genome-wide chromatin occupancy analysis reveals a role for ASH2 in transcriptional pausing. *Nucleic Acids Res* 39: 4628 – 4639
16. Ashburner M, Ball CA, Blake JA, Botstein D, Butler H, Cherry JM, Davis AP, Dolinski K, Dwight SS, Eppig JT *et al* (2000) Gene ontology: tool for the unification of biology. The Gene Ontology Consortium. *Nat Genet* 25: 25 – 29
17. Belacortu Y, Weiss R, Kadener S, Paricio N (2012) Transcriptional activity and nuclear localization of Cabut, the Drosophila ortholog of vertebrate TGF-beta-inducible early-response gene (TIEG) proteins. *PLoS ONE* 7: e32004
18. Ng M, Diaz-Benjumea FJ, Vincent JP, Wu J, Cohen SM (1996) Specification of the wing by localized expression of wingless protein. *Nature* 381: 316 – 318
19. Cook T, Gebelein B, Mesa K, Mladek A, Urrutia R (1998) Molecular cloning and characterization of TIEG2 reveals a new subfamily of transforming growth factor-beta-inducible Sp1-like zinc finger-encoding genes involved in the regulation of cell growth. *J Biol Chem* 273: 25929 – 25936
20. Kaczynski J, Cook T, Urrutia R (2003) Sp1- and Krüppel-like transcription factors. *Genome Biol* 4: 206
21. Spittau B, Krieglstein K (2012) Klf10 and Klf11 as mediators of TGF-beta superfamily signaling. *Cell Tissue Res* 347: 65 – 72
22. Subramaniam M, Harris SA, Oursler MJ, Rasmussen K, Riggs BL, Spelsberg TC (1995) Identification of a novel TGF-beta-regulated gene encoding a putative zinc finger protein in human osteoblasts. *Nucleic Acids Res* 23: 4907 – 4912
23. Chrisman HR, Tindall DJ (2003) Identification and characterization of a consensus DNA binding element for the zinc finger transcription factor TIEG/EGRalpha. *DNA Cell Biol* 22: 187 – 199
24. Brown JL, Grau DJ, DeVido SK, Kassis JA (2005) An Sp1/KLF binding site is important for the activity of a Polycomb group response element from the Drosophila engrailed gene. *Nucleic Acids Res* 33: 5181 – 5189
25. Oh H, Slattery M, Ma L, Crofts A, White KP, Mann RS, Irvine KD (2013) Genome-wide association of Yorkie with chromatin and chromatin-remodeling complexes. *Cell Rep* 3: 309 – 318
26. Goulev Y, Fauny JD, Gonzalez-Marti B, Flagiello D, Silber J, Zider A (2008) SCALLOPED Interacts with YORKIE, the Nuclear Effector of the Hippo Tumor-Suppressor Pathway in Drosophila. *Curr Biol* 18: 435 – 441
27. Peng HW, Slattery M, Mann RS (2009) Transcription factor choice in the Hippo signaling pathway: homothorax and yorkie regulation of the microRNA bantam in the progenitor domain of the Drosophila eye imaginal disc. *Genes Dev* 23: 2307 – 2319
28. Nicolay BN, Bayarmagnai B, Islam ABMMK, Lopez-Bigas N, Frolov MV (2011) Cooperation between dE2F1 and Yki/Sd defines a distinct transcriptional program necessary to bypass cell cycle exit. *Genes Dev* 25: 323 – 335
29. Oh H, Irvine KD (2011) Cooperative Regulation of Growth by Yorkie and Mad through bantam. *Dev Cell* 20: 109 – 122
30. Ferrigno O, Lallemand F, Verrecchia F, L'Hoste S, Camonis J, Atfi A, Mauviel A (2002) Yes-associated protein (YAP65) interacts with Smad7 and potentiates its inhibitory activity against TGF-beta/Smad signaling. *Oncogene* 21: 4879 – 4884
31. Sansores-Garcia L, Atkins M, Moya IM, Shahmoradgoli M, Tao C, Mills GB, Halder G (2013) Mask is required for the activity of the hippo pathway effector Yki/YAP. *Curr Biol* 23: 229 – 235
32. Sidor CM, Brain R, Thompson BJ (2013) Mask proteins are cofactors of Yorkie/YAP in the hippo pathway. *Curr Biol* 23: 223 – 228
33. Hamaratoglu F, Willecke M, Kango-Singh M, Nolo R, Hyun E, Tao C, Jafar-Nejad H, Halder G (2006) The tumour-suppressor genes NF2/Merlin and Expanded act through Hippo signalling to regulate cell proliferation and apoptosis. *Nat Cell Biol* 8: 27 – 36
34. Oh H, Irvine KD (2008) In vivo regulation of Yorkie phosphorylation and localization. *Development* 135: 1081 – 1088
35. Sun G, Irvine KD (2011) Regulation of Hippo signaling by Jun kinase signaling during compensatory cell proliferation and regeneration, and in neoplastic tumors. *Dev Biol* 350: 139 – 151
36. Kanehisa M, Goto S (2000) KEGG: kyoto encyclopaedia of genes and genomes. *Nucleic Acids Res* 28: 27 – 30